MGE-Like Neural Progenitor Cell Survival and Expression of Parvalbumin and Proenkephalin in a Jaundiced Rat Model of Kernicterus

Fu-Chen Yang[1], Jay L. Vivian[2], Catherine Traxler[1], Steven M. Shapiro[3], and John A. Stanford[1,4] (iD)

Abstract

Kernicterus is a permanent condition caused by brain damage from bilirubin toxicity. Dystonia is one of the most debilitating symptoms of kernicterus and results from damage to the globus pallidus (GP). One potential therapeutic strategy to treat dystonia in kernicterus is to replace lost GP neurons and restore basal ganglia circuits through stem cell transplantation. Toward this end, we differentiated human embryonic stem cells (hESCs) into medial ganglion eminence (MGE; the embryological origin of most of the GP neurons)-like neural precursor cells (NPCs). We determined neurochemical phenotype in cell culture and after transplanting into the GP of jaundiced Gunn rats. We also determined grafted cell survival as well as migration, distribution, and morphology after transplantation. As in the GP, most cultured MGE-like NPCs expressed γ-aminobutyric acid (GABA), with some co-expressing markers for parvalbumin (PV) and others expressing markers for pro-enkephalin (PENK). MGE-like NPCs survived in brains at least 7 weeks after transplantation, with most aggregating near the injection site. Grafted cells expressed GABA and PV or PENK as in the normal GP. Although survival was low and the maturity of grafted cells varied, many cells produced neurite outgrowth. While promising, our results suggest the need to further optimize the differentiation protocol for MGE-like NPC for potential use in treating dystonia in kernicterus.

Keywords

cell therapy, hyperbilirubinemia, transplantation, globus pallidus

Introduction

Kernicterus is caused by excessive neonatal hyperbilirubinemia. In severe neonatal jaundice, high levels of bilirubin exceed the binding capacity of blood albumin. Free unconjugated bilirubin crosses the blood–brain barrier and enters the brain where it causes neurotoxicity to selective nuclei including the globus pallidus (GP), subthalamic nucleus, inferior colliculus, cochlear, vestibular and oculomotor nuclei, hippocampus, and cerebellum[1–5]. Other brain regions are relatively spared[6–8]. Kernicterus is a permanent and devastating syndrome and the classic cause of dystonic cerebral palsy. Patients frequently have symptoms of intractable dystonia, prolonged episodes of painful status dystonicus, and can be virtually locked-in without movement but with normal cognitive function[2,3]. So far, there is no effective treatment for kernicteric dystonia[2].

Kernicteric dystonia is thought to be due to bilirubin toxic damage in the GP. Clinically, human magnetic resonance images[9–11] and autopsies[12] reveal bilateral lesions in the GP. Recently, our pilot study using the classical jaundiced (jj)

Gunn rat model of kernicterus demonstrated substantial neuronal loss in the GP of kernicteric rat brain[13]. It has been suggested that kernicteric dystonia is due to altered GP output, ultimately affecting input to downstream motor nuclei, leading to abnormal movements and muscle tone[14,15]. Targeting GP with neuronal stem cells to replace lost cells

[1] Department of Molecular and Integrative Physiology, The University of Kansas Medical Center, Kansas City, KS, USA
[2] Department of Pathology and Laboratory Medicine, The University of Kansas Medical Center, Kansas City, KS, USA
[3] Department of Neurology, The University of Kansas Medical Center, Kansas City, KS, USA
[4] Kansas Intellectual and Developmental Disabilities Research Center, The University of Kansas Medical Center, Kansas City, KS, USA

Corresponding Author:
John A. Stanford, Department of Molecular and Integrative Physiology, The University of Kansas Medical Center, Kansas City, KS 66160, USA.
Email: jstanford@kumc.edu

and restore damaged pathways is a potential therapeutic approach to alleviate dystonia in kernicterus.

One cell therapy approach is to design neuronal stem/progenitor cells (NSCs/NPCs) that specifically differentiate into the desired cell type for transplantation in neurodegenerative diseases for which the damaged neuron is known. Efforts include cells that resemble midbrain dopamine neurons for Parkinson's disease[16,17] and forebrain γ-aminobutyric acid (GABA) neurons for Huntington's disease[18,19]. Accordingly, we derived NPCs from the WA09 human embryonic stem cell line (hESC) and differentiated these cells into medial ganglion eminence (MGE)-like NPCs[20]. The MGE is the major embryologic origin of GP neurons[21,22]. In our previous study, we observed short-term (3 days–3 weeks) development of MGE-like NPCs after grafting into brains of non-immunosuppressed jaundiced (jj) and nonjaundiced (Nj) 21-day-old (P21) Gunn rats[20].

The Gunn rat model provides significant benefit for the research of neonatal jaundice and kernicterus[6]. Homozygous jaundiced Gunn (jj) rats lack the gene for uridine diphosphate glucuronosyltransferase (UGT1A1), the enzyme responsible for bilirubin conjugation and elimination. The jj rat pups become hyperbilirubinemic but have no or minimal symptoms of kernicterus. Injecting a sulfonamide (eg, sulfadimethoxine, or sulfa) during the postnatal hyperbilirubinemia period in the jj rat can produce kernicterus as sulfa competes with bilirubin for blood albumin-binding sites, thus promoting unbound bilirubin to move into the brain[4,5].

Given the fact that the brain environment changes with development, and that bilirubin may interact differently at different stages of development[3,23], long-term survival and appropriate development of the transplanted cells in this complicated situation would be imperative prerequisites for functional restoration. In this study, we utilized jj-sulfa model of kernicterus to investigate the survival and development of MGE-like NPCs transplanted into the GP of jj Gunn rats and their Nj littermates.

Methods

Preparation of Stem Cells for Transplantation

Pluripotent stem cell culture. WA09 human embryonic stem cells[24] were maintained in an undifferentiated state by culture on Matrigel in mTeSR Plus media (Corning 354277; Corning, Tewksbury, MA, USA). Cells were passaged every 4 days with GCDR (Gentle Cell Dissociation Reagent; STEMCELL Technologies, Vancouver, BC, Canada) ReLeSR reagent (Stem Cell Technologies 05872; STEMCELL Technologies).

Pluripotent stem cell aggregation and differentiation. Embryoid body (EB) formation and culture were performed in defined serum-free knockout serum replacement media

(KOSR)[25] which consisted of KO-MEM, 20% knockout serum replacement, glutamine, non-essential amino acids, and penicillin-streptomycin (all from Thermo Scientific, Waltham, MA, USA). The media was supplemented with small molecules and growth factors, including fibroblast growth factor (FGF), Rho-associated, coiled containing protein kinase inhibitor [ROCKi (Y27632)], LDN193189, SB431542, IWP3, fibroblast growth factor 8a (FGF8A), smoothened agonist (SAG), and DAPT. Cells were aggregated via centrifugation using AggreWell plates (Stem Cell Technologies) to a defined EB size of 2,100 cells. After overnight culture of the cells in AggreWell plates at 37°C, 5% CO_2, EBs were collected. These EBs were subsequently cultured in ultra-low attachment plates in supplemented KOSR media with small molecules at 37°C in 5% CO_2, modified from the previous studies[26]. Half of the media was replaced daily. On days in which the small molecule formula was changed, EBs were collected with strainers (37 μm pore size, Stem Cell Technologies) and moved to the appropriate media. After 18 days of differentiation, EBs were then transferred to neural maintenance media NTD2 (neurobasal media), 1× B27, 1× insulin-transferrin-selenium, 1× pyruvate, 0.5 μg/ml cAMP, 0.4 μg/ml ascorbic acid, 25 μM Basal Medium Eagle (BME), 25 μM glutamine (all from Thermo Scientific), and 10 ng/ml each of brain-derived neurotrophic factor (BDNF), glial cell line–derived neurotrophic factor (GDNF), ciliary neurotrophic factor (CNTF), and insulin-like growth factor (IGF)-1 (R&D Systems, Minneapolis, MN, USA).

Dissociation of embryoid bodies. EBs were collected on days 20 to 22 and placed into GentleMACS dissociation reagent (Miltenyi, Auburn, CA, USA) and dissociated at 37°C for 20 min, with gentle hand pipetting after 10 min. Dissociated cells were passed through a strainer, collected in NTD2 media, and counted. For continued culture, cells were plated onto laminin-coated coverslips in NTD2 media and cultured at 37°C in 5% CO_2. Before transplantation, cells were resuspended at 40,000 cells per 2.5 μl in NTD2 media supplemented with 30 ng/ml each BDNF, GDNF, CNTF, and IGF-1.

Animals

Male and female Gunn rats used in this experiment were bred in the University of Kansas Medical Center's colony by pairing homozygous (jj) males and heterozygous (Nj) females to produce litters of approximately 50% jj and 50% Nj Gunn rat pups. A total of 24 rats, 18 jj and 6 Nj, were used. Rats lived with their mothers and siblings before and after surgery and were weaned at 28 days of age (P28). Rats were housed in a temperature-controlled (23°C–25°C) and humidity-controlled (45%–50%) room maintained on 12/12-h light/dark cycles with food (Teklad laboratory animal diets 8604; Envigo, Madison, WI, USA) and water available *ad*

libitum. All experimental procedures were conducted in accordance with the Guide for the Care and Use of Laboratory Animals. The study was approved by the University of Kansas Medical Center's Institutional Animal Care and Use Committee.

## Bilirubin Level Measurement and Sulfa Injection

Total serum bilirubin (TSB) levels of all jj rats were measured at postnatal day 10 (P10; immediately before sulfa injection) and again at P20, 1 day before the NPC transplantation surgery. For each animal, about 50 μl of blood was taken and the TSB concentration was determined using a Leica Unistat bilirubinometer (Reichert Inc., Depew, NY, USA). Bilirubin levels in Nj rats were below 0.1 mg/dl, the limit of detection of the bilirubinometer. Six jj rats received a low dose of sulfadimethoxine (SulfaMed; Aspen Veterinary Resources Ltd., Liberty, MO, USA), 50 mg/kg, intraperitoneally, and another 12 received a high dose of sulfa, 70 mg/kg, intraperitoneally. This was based on our unpublished data that 80 mg/kg of sulfa is a critical dose to induce severe symptoms (eg, dystonia) of kernicterus with high mortality. We chose these two doses to lessen the loss of experimental animals.

Surgery for Cell Transplantation

At P21, jj rats and nonjaundiced littermates received WA09 human embryonic stem cells differentiated into GABAergic MGE-like NPCs into the GP. Animals were anesthetized with isoflurane (3%–4% for induction and 2%–2.5% for maintenance with oxygen) and placed in a stereotaxic frame (Kopf, Tujunga, CA, USA). A small hole on the skull was drilled over the GP using stereotaxic coordinates from a developing rat brain stereotaxic atlas[27]. The coordinates were 5.3 mm anterior and 2.8 mm lateral from the interaural midpoint. Suspended cells were taken from centrifuge vial kept at 4°C with a 26-gauge, 10 μl Hamilton microsyringe, the needle was then lowered to a depth of 5.0 mm from the brain surface, and 40,000 of NPCs suspended in 2.5 μl of NDT2 media were injected into the GP unilaterally at a speed of 0.5 μl/min. The needle was left in place for an additional 5 min to prevent efflux of cells and then slowly removed. After surgery, the scalp was sutured, and the rat was returned to its cage for recovery. All rats received ketoprofen 5 mg/kg subcutaneously immediately after surgery and for another 2 successive days. The immunosuppressant Cyclosporine A (10 mg/kg, sc, Sandimune Injection, 50 mg/ml, Novartic, Stein, AG; diluted with sesame oil; Sigma Life Science, St. Louis, MO, USA) was given 1 day before and 3 weeks after surgery; thereafter it was given orally by mixing in daily drinking water (50 μl/ml, diluted from Atopica oral solution 100 mg/ml; Elanco US Inc., Greenfield, IN, USA) until the end of the experiment.

Immunohistochemistry and Immunocytochemistry

At 3 weeks [short-term groups, three rats in 50 mg/kg (jj50S3W) and six rats in 70 mg/kg sulfa groups (jj70S3W)] or 7 weeks [long-term groups, three rats in 50 mg/kg (jj50S7W), six rats in 70mg/kg sulfa groups (jj70S7W), and six Nj rats (Nj7W)] after cell transplantation (ie, P42 and P70), rats were deeply anesthetized with isoflurane and transcardially perfused with ice-cold phosphate-buffered saline (PBS) followed with 4% paraformaldehyde (PFA; Sigma-Aldrich, St. Louis, MO, USA). Brains were removed, preserved in 4% PFA overnight, and then cryoprotected in 30% sucrose PBS solution prior to sectioning for immunohistochemistry (IHC) analyses. Coronal sections containing the graft and the GP were cut at 30 μm with a cryostat (Leica CM3050S; Leica Biosystems, Buffalo Grove, IL, USA). Brain sections were processed with standard floating section IHC methods: three washes with phosphate-buffered saline with Tween 20 (PBST), followed by 2 h of blocking in PBST containing 5% normal goat serum and 1% BSA, and then incubated with primary antibodies overnight at 4°C. Sections were then washed three times with PBS and incubated with secondary antibodies for 2 h. After three washes, sections were mounted using mounting media Fluromount-G (Southern Biotech, Birmingham, AL, USA) and coverslipped. For each brain, every sixth section was stained with mouse monoclonal antibody specific for human species cytoplasmic marker, STEM121 (1:500; Cellartis-Clontech-Takara Bio, Mountain View, CA, USA), to identify grafted human cells and alternatively double-stained with the following antibodies: rabbit anti-human Ku80 (1:500; ABCam, Cambridge, MA, USA) for human cell nuclei, rabbit anti-parvalbumin (PV, 1:500; Synaptic Systems, Göttingen Germany) to identify graft cells expressing PV, and rabbit anti-proenkephalin (PENK, 1:1,000; LifeSpan BioSciences, Seattle, WA, USA) for graft or host cells expressing PENK. A further set of 1:6 series sections was processed for double-staining of mouse anti-STEM123 [1:300; specific for human glial fibrillary acidic protein (GFAP)]; Cellartis-Clontech-Takara Bio) and Ku80. Cultured cells that were not used for transplantation were cultured for 6 days, then plated onto laminin and fixed. Immunocytochemistry (ICC) was performed to identify the cell properties. The following antibodies were used for ICC: mouse immunoglobulin G (IgG)2A anti-glutamic acid decarboxylase 6 (GAD-6, 1:100; Developmental Studies Hybridoma Bank, University of Iowa, Iowa City, IA, USA), rabbit anti-βIII-tubulin (1:200; ECM Bioscience, Versailles, KY, USA), rabbit-anti-PV (1:500; Synaptic Systems), rabbit anti-proenkephalin (PENK, 1:1000; LifeSpan BioSciences), and mouse anti-STEM123 (1:300; Cellartis-Clontech-Takara Bio). Immune reactions were visualized by corresponding secondary antibody labeling: goat anti-mouse IgG (H+L) Alexa Fluor 488 (1:1,000; Invitrogen, Waltham, MA, USA), goat anti-rabbit Alexa Fluor 555 (1:1,000; Invitrogen), and goat anti-mouse IgG2A Alexa Fluor 594 (1:1,000; Invitrogen).
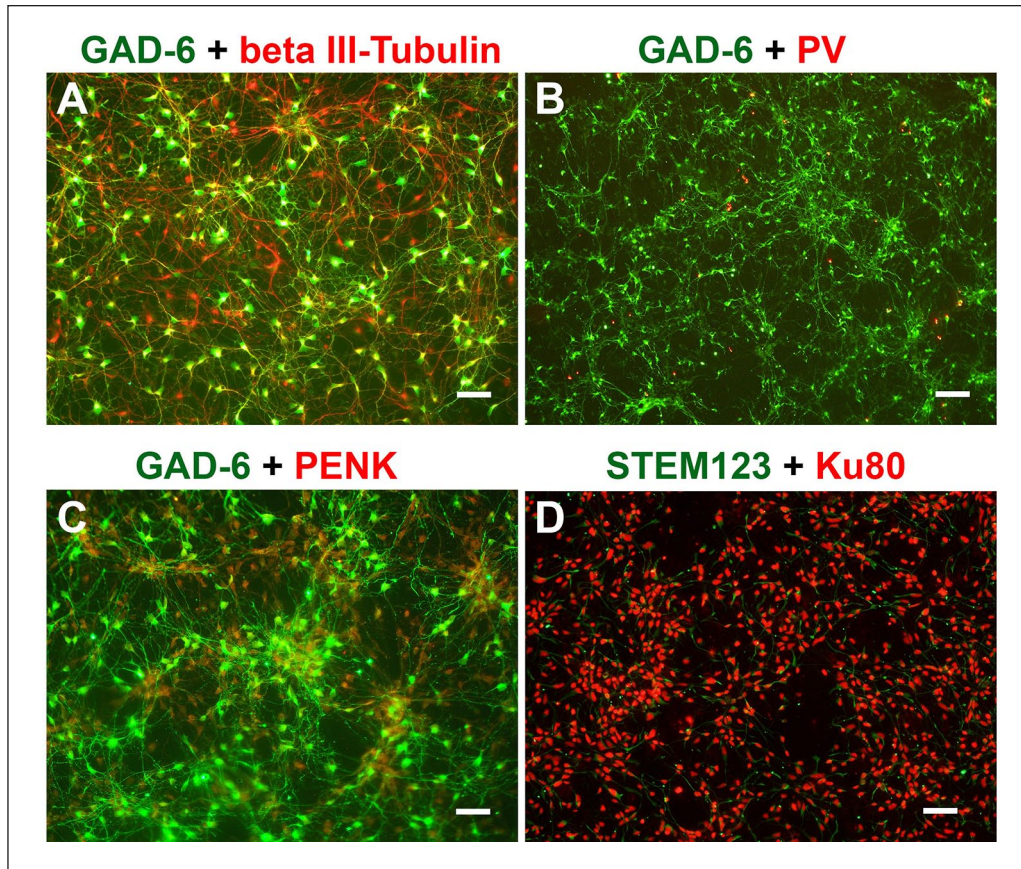
Figure 1. MGE-like NPCs expressed GAD-6, βIII-tubulin, PV, PENK, human Ku80, and STEM123 in culture. (A) Photomicrograph showing a large number of cells were GAD-6-ir and βIII-tubulin-ir, which indicated most cells had GABAergic neuronal phenotype. (B) GAD-6 and PV double labeling indicated a small group of GABAergic neurons also expressed PV. (C) ICC for GAD-6 and PENK suggested many cells were also PENK-ir. (D) Ku80 and STEM123 double-labeling revealed around 90% of NPCs expressed GFAP in culture. Note that rich extending entangled long fibers can be observed in the culture. Scale bar: A, C, D, 50 µm; B, 100 µm. MGE: medial ganglion eminence; NPCs: neural precursor cells; GAD-6: glutamic acid decarboxylase 6; PV: parvalbumin; PENK: pro-enkephalin; ICC: Immunocytochemistry; GFAP: glial fibrillary acidic protein.

## Cell Counting and Statistics

All sections were examined under a fluorescence microscope (Nikon Eclipse 80i; Nikon, Melville, NY, USA) and analyzed with CellSens Standard software (Olympus, Center Valley, PA, USA). Images (10×) of areas containing graft tissue were used for cell counting. Based on the STEM121 and Ku80 double-labeling, the numbers of viable transplanted cells were manually counted with CellSens or NIH ImageJ (NIH, Bethesda, MD, USA) independently by two people. The mean was multiplied by 6 to estimate the total number of viable cells. The proportion of astrocytes to the total surviving cells was quantified by comparing the STEM123 and Ku80 double-staining to the total Ku80-ir cells. The distribution distances of grafted cells from the graft tract were measured with CellSens Standard or NIH ImageJ based on the images of 10× magnification, and group differences were compared with analyses of variance (ANOVA; Systat 13.0; Systat Software Inc., San Jose, CA, USA). Cell survival rates between groups were analyzed using ANOVA, and Pearson's product–moment correlation was used for the correlation between bilirubin levels and graft cell survival rates. Bilirubin level changes in different groups and time points were also examined with ANOVA. Statistical significance was set at $P < 0.05$. All data are shown as mean $\pm$ standard error of the mean.

Results

Characteristics of the hESC-Derived MGE-Like NPCs

The NPCs used for transplantation were differentiated to GABAergic MGE neuron phenotypes based on our protocol modified from other study[26]. Cells further cultured 6 days after transplantation were examined with ICC to identify their neurochemical phenotype. *In vitro* ICC revealed that a large proportion of cells were GABAergic, as indicated by the expression of GAD-6. Cells with GAD-6 and βIII-tubulin colocalization were abundant (Fig. 1A). A small number of
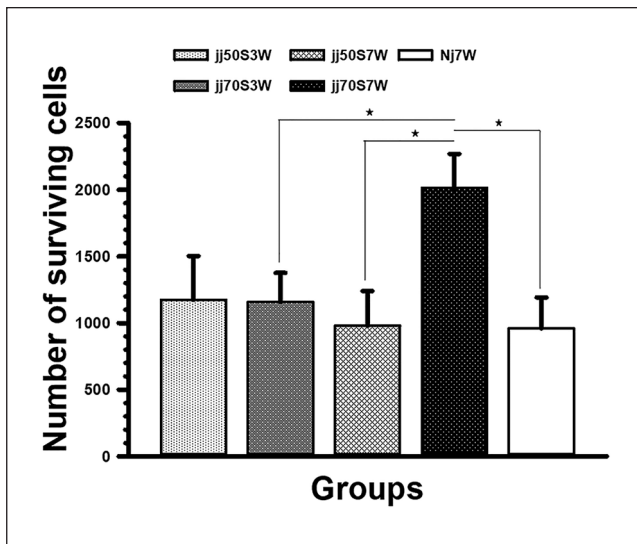
Figure 2. Survivability of grafted MGE-like NPCs in sulfa-treated jj rats and Nj control rats. Histogram indicates the number of surviving graft neurons in jj groups with 50 mg/kg or 70 mg/kg sulfa treatment and 3 weeks or 7 weeks of the surviving period after transplanting (jj50S3W, jj70S3W, jj50S7W, jj70S7W) and in Nj 7-week group (Nj7W). The jj70S7W group had a higher number of surviving cells (*$P = 0.007$ compared to Nj7W, *$P = 0.022$ compared to jj50S7W, *$P = 0.024$ compared to jj70S3W), about 2,000 cells, while all the other groups had about 1,000 of surviving graft cells. (mean $\pm$ SE). MGE: medial ganglion eminence; NPCs: neural precursor cells; jj: jaundiced; Nj: nonjaundiced.

cells co-expressed GAD-6 and PV, while quite a few were double-labeled with GAD-6 and PENK, indicating cells that differentiated into different phenotypes of GABAergic neurons (Fig. 1B, C). When cultured for 6 more days after EB dissociation, cells extending rich, entangled long fibers were observed. Ku80 and STEM123 double-staining also revealed that 92.5% $\pm$ 0.8% of NPCs had low to moderate levels of GFAP expression during this developmental stage (Fig. 1D).

Survival of MGE-Like NPC Grafts in Brain of Gunn Rats Treated With Low or High Dose of Sulfa 3 Weeks or 7 Weeks After Transplantation

Surviving cells were counted as Ku80-ir nuclei overlapped, were surrounded by, or were opposite to STEM121-ir cells. Cell survival rate was calculated as a percentage of the number of survival cells to the estimated total number of cells injected. Surviving graft cells were found in all brains, but one brain from the jj70S7W group was too damaged to get a full set of sections for cell counting. The number of surviving cells in each group is shown in Fig. 2. After excluding an outlier with an extreme number of surviving cells (7,944), the number of surviving cells in the jj70S7W group was significantly greater than all the other groups except the

jj50S3W, *post hoc* Fisher LSD (Least Significant Difference) method indicated $P = 0.007$ to Nj7W, $P = 0.022$ to jj50S7W, $P = 0.024$ to jj70S3W, and $P = 0.056$ to jj50S3W groups, while there were no differences among the other groups. Most of the grafted cells were in the GP/ic area, near the injection core. Surviving graft neurons exhibited abundant fiber outgrowth in every group. Figure 3 shows representative images of grafted neurons and fibers in jj and Nj groups. Necrotic tissue was identified in 8 of 17 jj brains and in 5 out of 6 Nj brains. Poor cell survival (total number $\leq$600) was found in 18% of jj and 50% of Nj brains and usually coincided with a larger amount of necrotic tissue (Fig. 6A, B).

### Bilirubin Level in jj Gunn Rats and Its Correlation with Grafted NPCs Survival

TSB concentration was 11.06 ± 0.24 mg/dl at P10, 12.31 ± 0.34 at P20. Pearson product–moment correlation revealed no correlations between the TSB levels and the survival rates of grafted NPCs either 3 weeks ($r = 0.0212$, $P = 0.957$), 7 weeks ($r = -0.022$, $P = 0.959$) after transplantation, or the overall survival rate ($r = 0.0865$, $P = 0.741$). Bilirubin levels for each group and time point are shown in Fig. 4. Total serum bilirubin was greater in the 50 mg/kg than in the 70 mg/kg sulfa-treated group at both time points ($F = 13.250$, $P < 0.01$). Bilirubin levels increased between P10 and P20 for both groups ($F = 20.495$, $P < 0.001$). There was not a significant interaction between groups and time on the measure.

### Distribution, Development, and Migration of Graft MGE-Like NPCs

The anterior–posterior distance of grafted cells distribution was defined as the presence of cells stained with both STEM121 and Ku80. Cell distribution distances, shown in Fig. 5, did not differ significantly between groups ($F = 1.298$, $P = 0.310$). Three weeks after transplantation, grafted cells generated many fibers. However, immature cells were also frequently observed (Fig. 6C). Although most grafted cells remained close to the graft core in the GP/internal capsule (ic) region, clusters of cells were found distributed into cortex, striatum, thalamus, fornix, and septal area (Fig. 6D). Cell migration is usually limited within 500 μm from the core (measured as a straight line from the cell body to the core of the graft on the same plane). Cell migration over longer distances, for example, 1,000 μm, was also observed (Figs. 6E and 7C). Well-surviving grafts were large in size, containing hundreds of cells in one section. Poor-surviving grafts usually had a large volume of necrotic cells (Fig. 6A and B).

### Neurite Outgrowth, Pattern, and Distribution

Outgrowth fibers distributed densely near the injection site and spread a wide range in the host brain; the anterior–posterior distribution was about 100 to 180 μm further than the
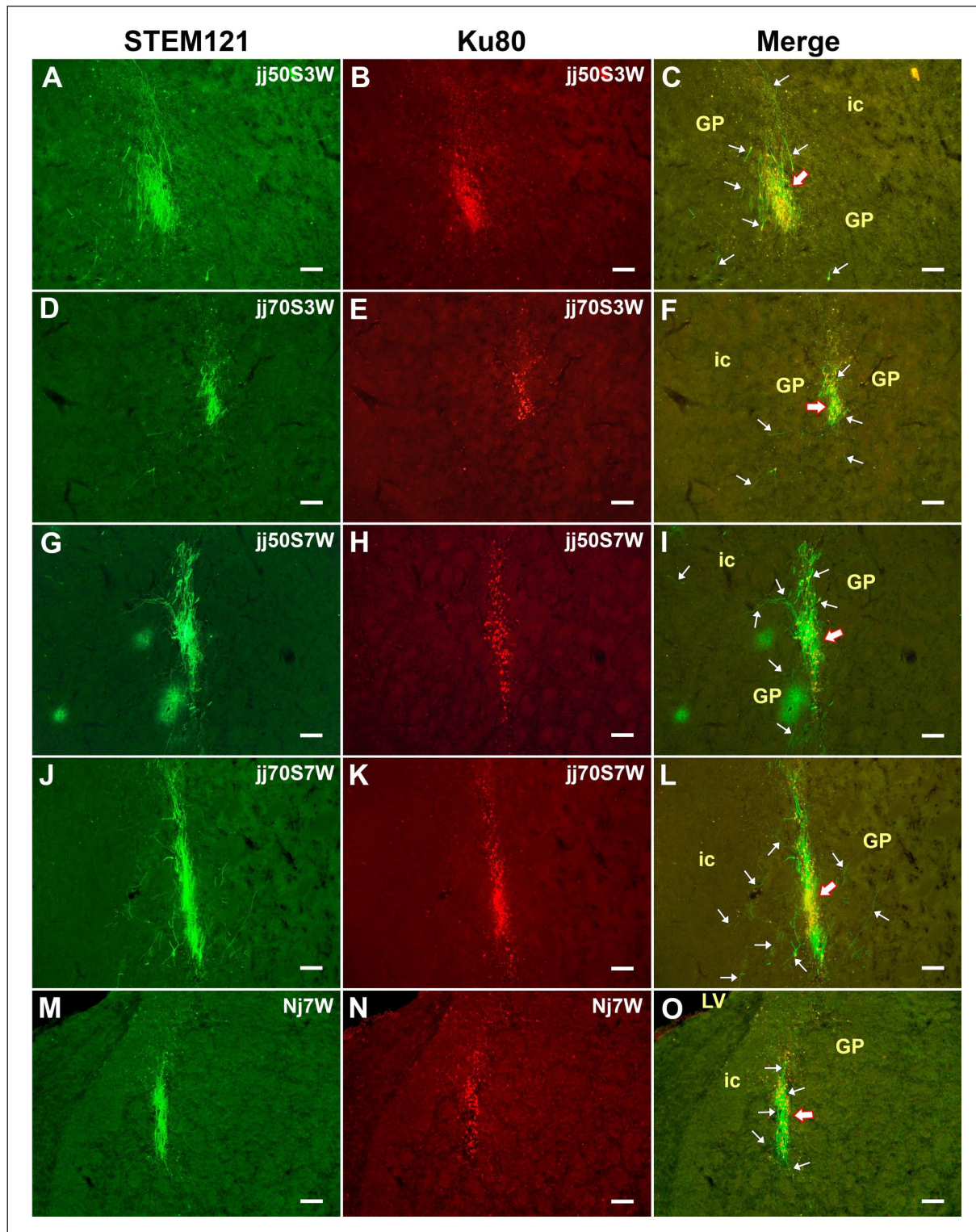
Figure 3. Survival and fiber outgrowth of grafted MGE-like NPCs in sulfa-treated jj rat and control Nj rat brains. Immunofluorescent (IF) staining for STEM121 (Alexa Fluor 488) and Ku80 (Alexa Fluor 555) confirmed the survival of MGE-like NPC grafts in the GP and ic regions of the host brains. Representative photos for each group are as follows: (A–C) jj50S3W; (D–F) jj70S3W; (G–I) jj50S7W; (J–L) jj70S7W, and (M–O) Nj7W. Outgrowth fibers are distributed densely near the graft core; long fibers frequently projected in ventromedial and medial directions. Some cells migrated from the core graft were also observed. For all photos, white arrow with red outline indicates the graft core, white arrows point to representative cells and fibers. Scale bar: 100 μm. MGE: medial ganglion eminence; NPCs: neural precursor cells; jj: jaundiced; Nj: nonjaundiced; GP: globus pallidus; ic: internal capsule; LV: lateral ventricle.
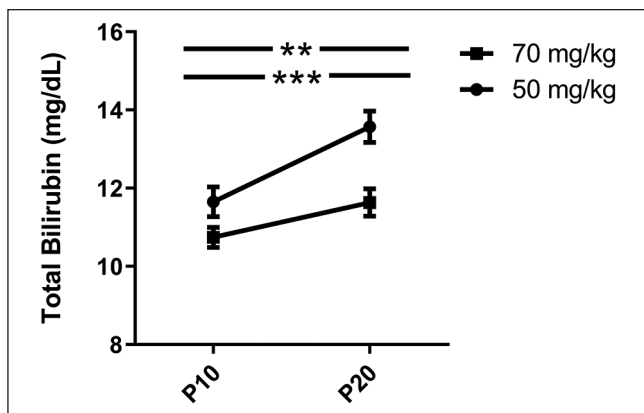
Figure 4. Total serum bilirubin levels of jaundiced rats at P10 and P20. Bilirubin levels were measured at P10, before either 50 mg/kg or 70 mg/kg of sulfa injection, and remeasured at P20, 1 day before the transplantation surgery. Serum bilirubin levels were greater in the 50 mg/kg group than in the 70 mg/kg group (**$P < 0.01$) and increased between P10 and P20 in both groups (***$P < 0.001$). Although bilirubin levels were within the normal range for this rat model, total serum bilirubin does not reflect the bilirubin concentration in the central nervous system (CNS). (mean ± SE).
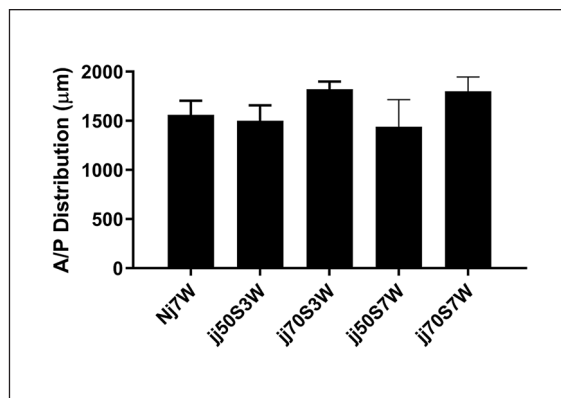
Figure 5. Anterior-posterior distribution of grafted MGE-like NPCs in the brains of sulfa-treated jj rats and Nj controls. The bar graph indicates the anterior-posterior span in μm where grafted cells were identified in the host brains of jj50S3W, jj70S3W, jj50S7W, jj70S7W, and Nj7W groups. The extent of cell distribution was about 1,500 μm to 1,820 μm and did not differ significantly between-groups. (mean ± SE). MGE: medial ganglion eminence; NPCs: neural precursor cells; jj: jaundiced; Nj: nonjaundiced.
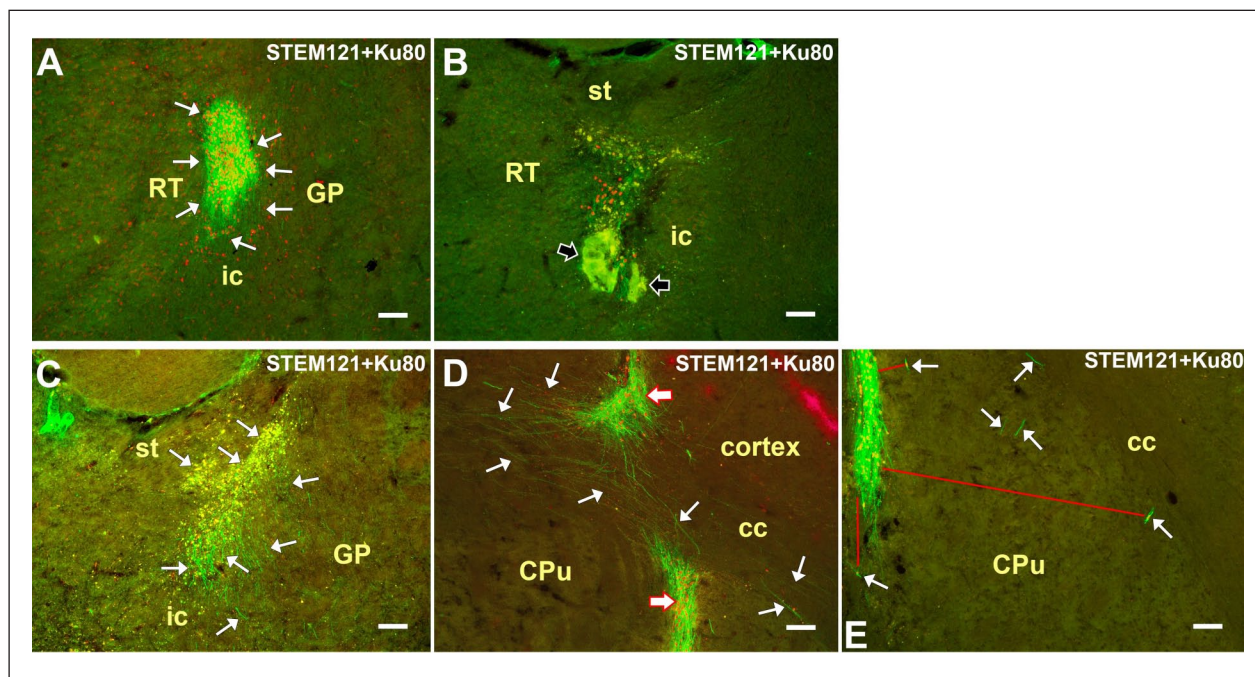
Figure 6. Graft cells development, distribution, and migration in the host brain indicated by IHC staining for STEM121 (Alexa Fluor 488) and Ku80 (Alexa Fluor 555). (A) Photomicrograph showing a hypertrophic graft located in the ic, RT region, containing hundreds of cells and numerous fibers. Survivability of this graft was 19.9%. (B) a low survival rate graft contained clusters of necrotic tissue. Both A and B were brains of jj70S7W group. (C) Three weeks after transplantation, a large cluster of immature graft cells were located in the ic. In the same graft, more matured cells sent large number of fibers toward the GP direction. (D) Two large grafts extended from the cortex, past the cc, to the striatum. Note abundant cells and fiber distribution. This type of graft and fiber distribution were frequently observed in 3- or 7-week groups. (E) Showing 7 weeks after transplantation, a graft in the striatum, extending to the GP. Cells migrated from the graft core for a long distance. Some fibers can be detected projecting away from the graft core also. White arrow with red outline indicates the graft core, black arrow with white outline indicates necrotic graft, white arrows point to representative cells and fibers, red line shows the distance of cell migration. Scale bar: 100 μm. IHC: immunohistochemistry; ic: internal capsule; RT: reticular nucleus of the thalamus; GP: globus pallidus; st: stria terminalis; cc: corpus callosum; CPu: caudate-putamen.
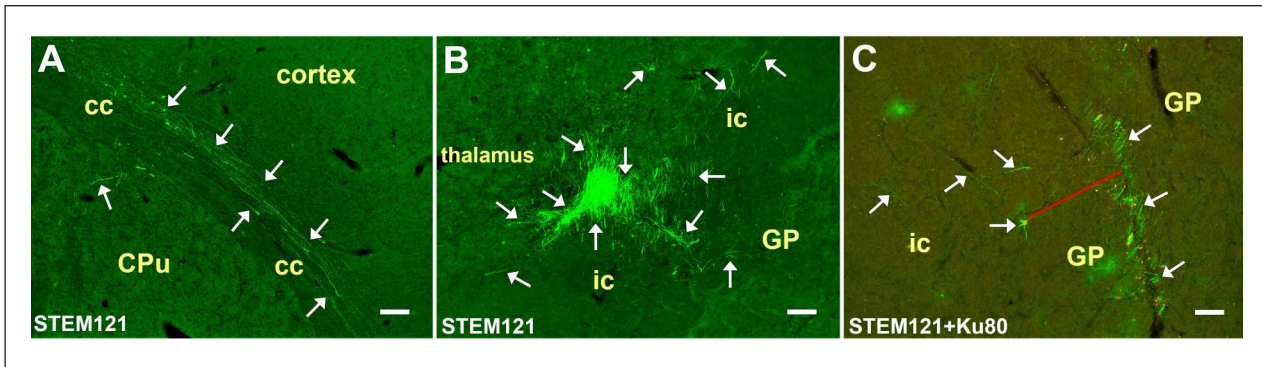
Figure 7. Graft neurite outgrowth patterns and distribution. (A) STEM121 labeling showing graft generated long projection fibers grew into corpus callosum and traveled a very long distance in the brain of a jj70S7W rat. (B) ICC of STEM121 indicated there were a large amount of short parallel fibers aggregated in the graft and some long, thin axons with collaterals projected to the GP in a jj50S3W brain. (C) STEM121 and Ku80 labeling in a jj70S7W brain showing the ventral end of a graft located in the GP. The graft had a very distinct pattern of parallel fibers, outgrowing long projection axons, and migrated neuron. White arrows point to representative cells and fibers, and red line shows the distance of cell migration. Scale bar: 100 μm. ICC: Immunocytochemistry; GP, globus pallidus; cc: corpus callosum; ic: internal capsule; CPu: caudate-putamen.

cell distribution. Most fibers were in the GP and ic. Many fibers of the core graft extended to the bed nucleus of the stria terminalis (BNST), the stria terminalis (ST), the reticular nucleus of the thalamus (RT), and the septal areas. For the dorsal part of the graft, fibers spread into the cortex and frequently traveled a long distance along the corpus callosum (cc) (Fig. 7A). Two patterns of fibers were observed frequently. One type was short, thick fibers, which extended in the same direction, resulting in the appearance of parallel fibers (Fig. 7B, C). The other type was long, thin axons that projected a long distance, including into the thalamus or further near entopeduncular nucleus (Fig. 7B, C).

Parvalbumin Expression in MGE-Like NPC Grafts

IHC labeling for PV and STEM121 indicated PV-ir neurons present in the graft tissue of sulfa-injected rats in all groups. However, there were very few PV-ir neurons found in 3-week groups. Seven weeks after transplantation, greater numbers of PV-ir neurons were identified (Fig. 8), and the number of cells was greater than in culture (Fig. 1B). These PV-ir neuron-containing grafts were found in the GP, ic, and some grafts extended to the RT areas.

PENK Expression in MGE-Like NPC Grafts

IHC of PENK and STEM121 double labeling indicated a small population of PENK-ir neurons in the graft as early as 3 weeks after grafting; these cells were small and immature with no neurites. In the 7 weeks post-transplantation brains, the well-surviving grafts contained PENK-ir cells that were more mature and had some neurites (Fig. 9A–C). Despite the substantial number of PENK-ir cells and processes we observed *in vitro*, the number of PENK-ir neurons *in vivo* was few and they were relatively immature (Fig. 1C).

PENK Expression in the Host Brain

MGE-like NPC grafts induced strong PENK expression in cells of the host brain. These PENK-ir cells presented near, or surrounding the graft site, but frequently left a zone with low PENK expression between the graft and the surrounding PENK-ir cells (Fig. 9D–F). This was predominantly observed in 3-week post-transplantation brains.
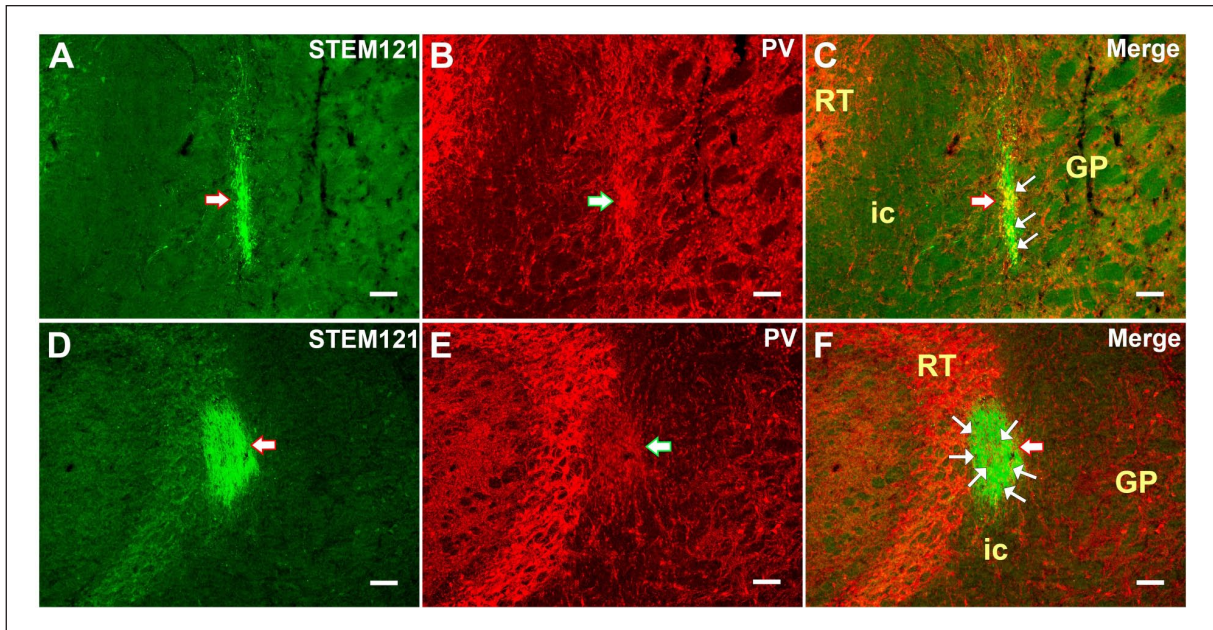
GFAP Expression in the MGE-Like NPC Grafts

IHC double-labeling for STEM123 and Ku80 revealed a very small population of human GFAP-expression cells in grafts from two brains in the 7-week group, estimated to be 0.76% and 1.1% of all surviving graft cells, indicating that a very small number of NPCs differentiated into astrocytes after grafting into rat brains. These cells were well-developed with many large cell processes extending into the graft cell cluster (Fig. 10).

Discussion

We recently reported that hESC-derived MGE-like NPCs were able to survive and generate an abundant number and variety of fibers 3 weeks after transplanting into the brains of jj Gunn rats[20]. In the current experiment, we advanced these findings to investigate long-term graft survival in the brains of cyclosporine A-treated jj rats that were injected with sulfa as neonates to induce a more severe condition of bilirubin toxicity that closely resembles kernicterus in human cases.

Excess NPCs harvested before transplantation were replated and grown *in vitro* for 6 more days, then examined with ICC double labeling of GAD-6 and βIII-tubulin. We confirmed that most of the cells in the culture were GABAergic neurons. ICC for PV and GAD-6 staining indicated a small

Figure 8. PV expression in the grafted MGE-like NPCs. Positive IHC staining of STEM121 and PV indicates the presence of PV neurons in grafted MGE-like NPC population 7 weeks after transplantation in 70 mg/kg sulfa-treated jj rat brains. (A–C) Graft located in the GP, PV-ir neurons aggregated into small groups. (D–F) Abundant of small size PV-ir neurons presented in a graft located in the ic. Note these cells were not as bright as those PV neurons in the host GP. Although there were numerous fibers, as most of these fibers were not labeled with PV, we cannot judge whether they were all generated from PV neurons. White arrow with red outline indicates the graft core, white arrow with green outline indicates PV-ir neuron group in the graft core, and white arrows point to representative cells. Scale bar: 100 μm. PV: parvalbumin; MGE: medial ganglion eminence; NPCs: neural precursor cells; IHC: Immunohistochemistry; GP, globus pallidus; ic: internal capsule; RT: reticular nucleus of the thalamus.
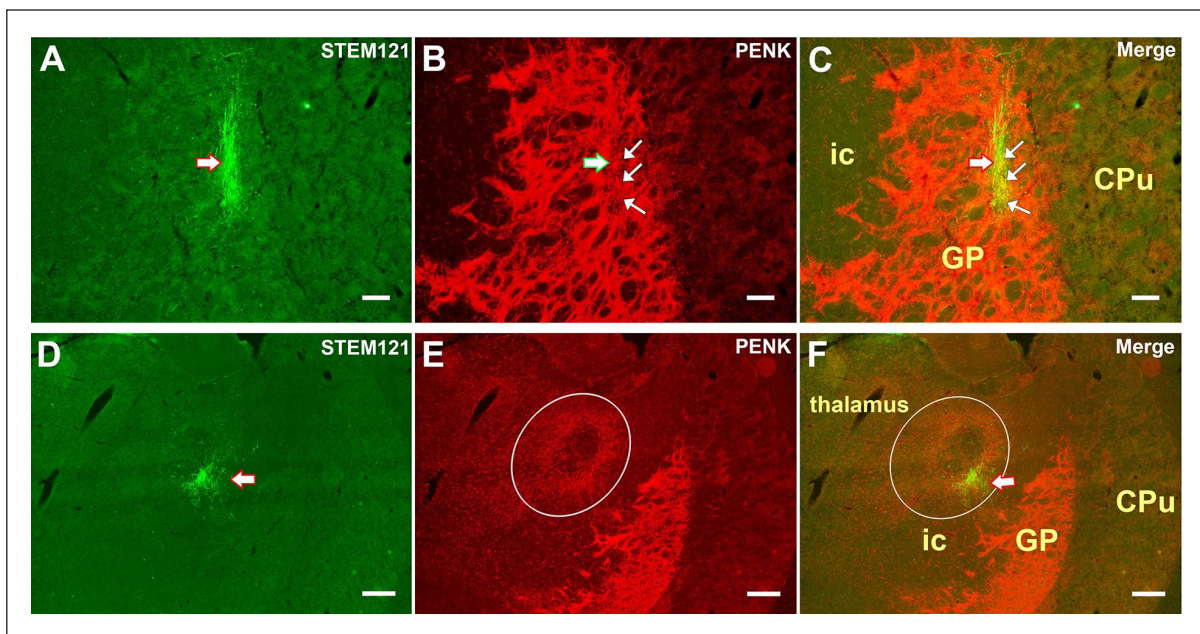
Figure 9. PENK expression in the graft and the host brain. (A–C) STEM121 and PENK co-labeling showing PENK-ir neurons presented in a graft located in the GP of a jj70S3W brain. (D–F) Photomicrograph showing graft in a jj50S3W brain, located in the ic, having fibers extended to the GP. The graft activated strong PENK-expressing in a group of host astrocytes that surrounded the graft, leaving a low PENK-expression zone between the graft and the surrounding PENK-ir astrocytes. White arrow with red outline indicates the graft core, white arrow with green outline indicates PENK-ir neuron group in the graft core, white arrows point to representative cells, and white circle indicates the area of PENK-hyper-expression. Scale bar: A–C, 100 μm; D–F, 200 μm. PENK: pro-enkephalin; GP, globus pallidus; ic: internal capsule; CPu: caudate-putamen.
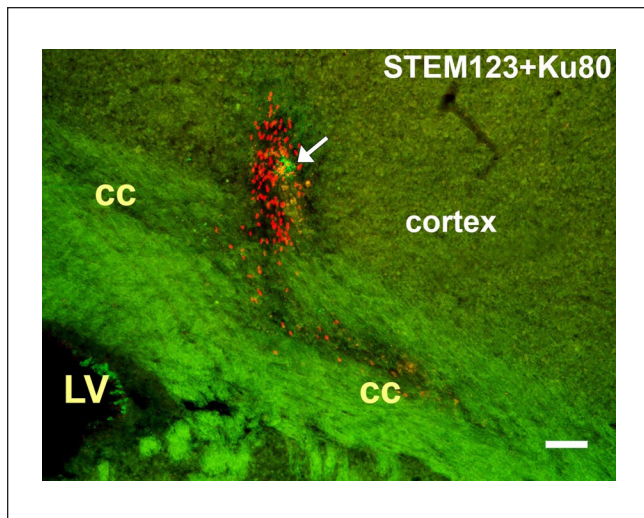
Figure 10. STEM123 (human GFAP) expression in the graft NPCs. Photomicrograph showing one grafted cell expressed GFAP, which indicated this cell differentiated into astrocytes. This cell was well-developed with cell processes extending into the graft cell cluster. White arrow points to the GFAP-ir cell. Scale bar: 100 μm. GFAP: glial fibrillary acidic protein; NPCs: neural precursor cells; cc: corpus callosum; LV: lateral ventricle.

population of GABAergic neurons co-expressed PV as previously reported[20,26]. Consistent with our recent study, many cells also co-expressed PENK and GAD-6. MGE is the main embryonic origin of PV-ir GABA neurons[21,22,28], while the lateral ganglionic eminence (LGE) is progenitor pool of PENK-ir GABA neurons[21,22]. The presence of PENK-ir neurons in our sample suggests that some LGE-like NPCs were generated by our protocol. These cells arise close in proximity in the embryo, and it is difficult to mimic small, localized differences in signaling *in vitro*. Alternatively, it is also possible this resulted due to species differences regarding cell phenotypes that arise from MGE. ICC labeling for Ku80 and STEM123 showed a high percentage of cultured cells expressing low levels of GFAP. This is consistent with previous reports of neural progenitors expressing GFAP during the early stages of development prior to maturing as neurons[29–31].

Graft survival is essential in transplantation, especially for reconstructing neural circuits. In this experiment, surviving grafts were identified in all transplanted brains, but the survival rate (percentage of surviving cells from the number of grafted cells) was not high (groups ranged between 2.5% and 5%). These rates were similar to that of the 3-week group (2.7%) in our previous study using the NPCs without immunosuppressant[20]. This suggests that cyclosporine A has little effect in these grafts or that its effect was similar to that of slightly elevated bilirubin levels as we observed in our previous study[20]. We attributed these effects bilirubin's antioxidant and immunosuppressant effects[32,33]. There were fewer cases of necrotic cells in jj brains than in Nj brains, which further suggested the endogenous antioxidative and

immunomodulation effects of bilirubin may be superior to cyclosporine A. Our results are consistent with a previous study reporting that cyclosporine A did not protect xenogeneic neural grafts effectively[34]. Cell survival may be improved by adding drugs such as prednisolone or pretreating cells with recipient serum[35].

Neither the baseline TSB level nor the TSB level 1 day before transplantation correlated with graft survival. TSB does not, however, reflect the free bilirubin concentration in the brain[36]. Our baseline TSB at P10 was within the range of that of similarly aged jj pups in the Gazzin et al[36] study. After sulfa injection, TSB levels decline sharply and then gradually return to previous levels over several days[36]. It is believed that elevated unbound free bilirubin in the brain accounts for decreased TSB levels in the hours and days following sulfa administration. At P20, the day before cell transplantation surgery, the TSB of all jj rats had returned to normal range or even slightly higher than the average value in other studies[5,6] and in our unpublished records. This suggests that unbound free bilirubin levels in the brain had declined by the time NPCs were grafted. Although there were some differences in bilirubin levels between dosing groups, these differences were small, and within the range of normal bilirubin concentration variation. We did not find significant differences between these two doses regarding graft survival and development.

Graft cells and fibers, identified by STEM121 and Ku80 staining, were located in areas along the injection tract. While the majority of grafts were in the GP and ic region, clusters of various sizes were found in cortex, striatum, reticular nucleus of the thalamus, fornix, and septal area. This distribution was similar to what we reported in our previous study[20]. Both 3-week and 7-week grafts contained cells in an immature neuroprogenitor state, with small or no cell processes. These cells could be primarily grafted or newly proliferated. A similar condition of proliferation has been reported in other studies transplanting hESC-derived NPCs to mice brains[37] or NSC in rat Huntington's model[18]. Our previous study[20] reported immature cells in the enlarged graft track that was full of Matrigel. In this experiment without Matrigel, the immature cells were found in the host parenchyma, gathered into clusters, neighboring, and inextricable to the matured cells that already had long fiber outgrowths, suggesting a better graft–host integration. Although most of the graft cells indicated limited migration (usually within 500 μm from the core), some cells were able to migrate a long distance (as far as 1,000 μm), as shown in Fig. 6E. Differences in migration might depend on individual NPC phenotype and appropriate extracellular guidance cues from the host brain.

Abundant outgrowth fibers generated from the graft neurons were observed. As reported in the previous study[20], at least two distinct patterns of fibers were detected. The short and thick parallel fibers usually found close to cell bodies resembled the dendrites of PV neurons in the GP[38]. These

neurons receive PENK projections from the striatal medium-size spiny neurons and send axons to the targets subthalamic nucleus, entopeduncular nucleus, and substantia nigra[39–41]. Another type was characterized as long, thin axons projecting a long distance, frequently to the internal capsule, thalamus, or along the corpus callosum if the graft neurons were located in the cortex or striatum.

While there were limited number of PV-expressing cells in the 6-day culture, co-labeling of STEM121 and PV indicated more abundant and mature PV neurons 7 weeks than 3 weeks after grafting. PV expression had been identified in a very small number of graft neurons as early as 3 days after transplantation, but these cells were immature and remained in Matrigel-containing injecting tract[20]. Despite the more abundant and mature PV neurons in the 7-week group, the immunoreactivity was not as strong as PV neurons in host GP. The labeled graft PV neurons were smaller, resembling PV neurons in the striatum. This suggested that grafted cells may require more time to develop or the current methods of cell differentiation need to be improved to increase the potential of producing more GP-like PV neurons. There are two main types of neurons in the GP. The MGE-originated PV neurons, or prototypic neurons, compose more than 60% of the GP neurons and form the GP descending pathways to the entopeduncular nucleus (EPN), thalamus, STN, and SN. The LGE-originated PENK neurons, or arkypallidal neurons, make up around 25% of GP neurons, which send feedback to the striatum[21,22,39,42]. It has been suggested that destroying the output of the GP would reduce inhibitory input to the motor thalamus, and disinhibition of the thalamus leads to the excessive movements of dystonia in kernicterus[14,15]. PV neurons are lower in the GP of kernicterus patients[12]. Our preliminary experiment also showed neonatally sulfa-treated jj rats had around 50% fewer PV neurons in the GP[13]. Thus, damage to PV neurons may be the main cause of dystonia in kernicterus, and the proper type of functional PV neurons should be critical for cell therapy in kernicterus.

PENK-ir neurons were identified in grafts of jj and Nj brains. Although there were large numbers of PENK-ir cells *in vitro*, they were few and relatively immature *in vivo*. The presence of PENK-ir neurons in the graft suggested the differentiating procedure might derive MGE-like and some LGE-like NPCs due to the difficulty of modulating the combination of expression patterns of transcription factors[21,22,26]. As GP normally contains LGE-originated PENK-ir neurons, PENK-ir neurons in the graft may facilitate the graft integration with the host brain, as it better resembles the heterogeneous environment of the GP.

MGE-like NPC graft activated strong PENK expression in cells of the host brain. These PENK-hyper-expressing cells surrounding the graft were predominantly observed in brains 3 weeks or shorter period post-transplantation, as we reported earlier[20]. This response was found in both jj and Nj brains, regardless of sulfa injection or not; thus, it was unlikely related to brain bilirubin levels. The presence of immunosuppressant did not affect this PENK expression, suggesting it may not be an immune response. Although it was known that astrocytes can express PENK in response to immune factors[43], PENK expression in the astrocytes has been proposed for modulating the growth and migration of opioid receptor-expression neurons of the nervous system[44,45]. PENK was considered a negative tropic regulator for neuronal proliferation and differentiation[44]. It is possible that PENK hyper-expression transiently after transplantation in the host brain is caused by PENK-expressing astrocytes which guided or prevented graft cells from further development and migration. This hypothesis needs to be tested.

Despite the low level of GFAP expressed in most of the NPCs during culture, very few cells differentiated into astrocytes after transplantation. This result again confirmed the majority of the hESCs differentiated into neurons using our protocol[20,46] and agree with *in vivo* studies reporting that some types of neural progenitors express GFAP during early developmental stages before maturing into neurons[29–31]. It was also reported that MGE-derived cells exhibited very limited or no GFAP after transplantation[28,47]. Moreover, in agreement with our previous study[20], STEM123-ir cells were not found in the graft 3 weeks after surgery, but only identified in the grafts after 7 weeks of transplantation. This suggests that if this type of NPCs differentiated into astrocytes, the development was very delayed compared with those which differentiated into neurons.

MGE progenitors have been applied for transplantation in disease models such as epileptic seizure[48] and stroke[49]. Usually, fresh embryonic cells or primary cultured cells are preferred for these studies. It has been criticized that human stem cell–derived MGE-like cells exhibit little migration and do not differentiate into subtypes seen in embryonic MGE progenitors[47]. In our experience, limited migration and delayed development were observed. These adverse conditions seem to be common in many studies using hESC or hNSC for transplantation[18,37,50,51]. Similar results followed stem cell transplantation for Parkinson's disease until studies revealed the midbrain dopamine neurons were only generated from the floor plate region. This resulted in successful new differentiation protocols[16,19]. Similarly, for MGE-derived PV-expressing progenitors for GP transplantation, a refined differentiation protocol that recapitulates MGE subdivisional neurodevelopment and efficiently generates these progenitors should be essential for further development in this field.

A high risk of tumor formation has been attributed to hESC-derived cells[51,52]. There were no signs of teratoma in our grafted rat brains. The risk of teratomas may be related to differentiation protocol. One study found that rats grafted with hESCs predifferentiated *in vitro* for 16 days developed severe teratomas, but if hESCs predifferentiated for 20 days or longer, the grafts were healthy[53]. In our protocol, hESCs were differentiated for 20–22 days, which may be essential for preventing teratoma formation after transplantation.

In conclusion, the present study demonstrated that MGE-like NPCs survived in brains after hyperbilirubinemia exacerbation for at least 7 weeks and were able to generate different types of fibers. In general, the graft survival rates were not high, but there was no difference between jj and Nj groups, which suggested cyclosporine A promoted graft survival in Nj brains, but it did not exert additional protection for grafts in the jj brains. Regardless of the period after grafting, most of the graft cells aggregated near the injection site with little extensive migration. While some cells appeared mature, some were small and immature. Small populations of graft cells expressed major neuropeptides PV and PENK as in the normal GP. These results suggested that while there is potential to use MGE-like NPC for cell therapy in kernicterus, there are still many aspects to be improved, including optimizing the differentiation protocol to reliably generate appropriate NPCs for transplantation.

Acknowledgments

Ethical Approval

This study was approved by the University of Kansas Medical Center's Institutional Animal Care and Use Committee (protocol #2019-2506).

Statement of Human and Animal Rights

All procedures in this study were conducted in accordance with the University of Kansas Medical Center's Institutional Animal Care and Use Committee's (2019-2506) approved protocols.

Statement of Informed Consent

There are no human subjects in this article and informed consent is not applicable.

Declaration of Conflicting Interests

The author(s) declared no potential conflicts of interest with respect to the research, authorship, and/or publication of this article.

Funding

ORCID iD

John A. Stanford https://orcid.org/0000-0002-4667-4057

References

1. Watchko JF, Tiribelli C. Bilirubin-induced neurologic damage—mechanisms and management approaches. N Engl J Med. 2013;369(21):2021–30.
2. Le Pichon JB, Riordan SM, Watchko J, Shapiro SM. The neurological sequelae of neonatal hyperbilirubinemia: definitions, diagnosis and treatment of the kernicterus spectrum disorders (KSDs). Curr Pediatr Rev. 2017;13(3):199–209.
3. Shapiro SM. Bilirubin toxicity in the developing nervous system. Pediatr Neurol. 2003;29(5):410–21.
4. Rose AL, Wisniewski H. Acute bilirubin encephalopathy induced with sulfadimethoxine in Gunn rats. J Neuropathol Exp Neurol. 1979;38(2):152–64.
5. Schutta HS, Johnson L. Clinical signs and morphologic abnormalities in Gunn rat treated with sulfadimethoxine. J Pediatr. 1969;75(6):1070–79.
6. Johnson L, Sarmienyo F, Blanc WA, Day. Kernicterus in rats with an inherited deficiency of glucuronyl transferase. AMA J Dis Child. 1959;97(5, pt 1):591–608.
7. Schutta HS, Johnson L. Bilirubin encephalopathy in the Gunn rat: a fine structure study of the cerebellar cortex. J Neuropathol Exp Neurol. 1967;26(3):377–96.
8. Jew JY, Sandquist D. CNS changes in hyperbilirubinemia. Functional implications. Arch Neurol. 1979;36(3):149–54.
9. Yilmaz Y, Alper G, Kiliçoglu G, Celik L, Karadeniz L, Yilmaz-Değirmenci S. Magnetic resonance imaging findings in patients with severe neonatal indirect hyperbilirubinemia. J Child Neurol. 2001;16(6):452–55.
10. Sugama S, Soeda A, Eto Y. Magnetic resonance imaging in three children with kernicterus. Pediatr Neurol. 2001;25(4): 328–31.
11. Govaert P, Lequin M, Swarte R, Robben S, De Coo R, Weisglas-Kuperus N, De Rijke Y, Sinaasappel M, Barkovich J. Changes in globus pallidus with (pre)term kernicterus. Pediatrics. 2003;112(6, pt 1):1256–63.
12. Hachiya Y, Hayashi M. Bilirubin encephalopathy: a study of neuronal subpopulations and neurodegenerative mechanisms in 12 autopsy cases. Brain Dev. 2008;30(4):269–78.
13. Yang FC, Stanford JA, Shapiro SM. Selective loss of parvalbumin expressing GABAergic neurons in the globus pallidus of an animal model of dystonic kernicterus. International Child Neurology Association and Child Neurology Society Conjoint Meeting; 2020 Oct 19–23; San Diego, CA.
14. Johnston MV, Hoon AH Jr. Possible mechanisms in infants for selective basal ganglia damage from asphyxia, kernicterus, or mitochondrial encephalopathies. J Child Neurol. 2000; 15(9):588–91.
15. Shapiro SM. Definition of the clinical spectrum of kernicterus and bilirubin-induced neurologic dysfunction (BIND). J Perinatol. 2005;25(1):54–59.
16. Kriks S, Shim JW, Piao J, Ganat YM, Wakeman DR, Xie Z, Carrillo-Reid L, Auyeung G, Antonacci C, Buch A, Yang L, et al. Dopamine neurons derived from human ES cells efficiently engraft in animal models of Parkinson's disease. Nature. 2011;480(7378):547–51.

17. Wakeman DR, Hiller BM, Marmion DJ, McMahon CW, Corbett GT, Mangan KP, Ma J, Little LE, Xie Z, Perez-Rosello T, Guzman JN, et al. Cryopreservation maintains functionality of human iPSC dopamine neurons and rescues Parkinsonian phenotypes in vivo. Stem Cell Rep. 2017;9(1):149–61. doi:10.1016/j.stemcr.2017.04.033.

18. McBride JL, Behrstock SP, Chen EY, Jakel RJ, Siegel I, Svendsen CN, Kordower JH. Human neural stem cell transplants improve motor function in a rat model of Huntington's disease. J Comp Neurol. 2004;475(2):211–19.

19. Ma L, Hu B, Liu Y, Vermilyea SC, Liu H, Gao L, Sun Y, Zhang X, Zhang SC. Human embryonic stem cell-derived GABA neurons correct locomotion deficits in quinolinic acid-lesioned mice. Cell Stem Cell. 2012;10(4):455–64.

20. Yang FC, Draper J, Smith PG, Vivian JL, Shapiro SM, Stanford JA. Short term development and fate of MGE-like neural progenitor cells in jaundiced and non- jaundiced rat brain. Cell Transplant. 2018;27(4):654–65.

21. Nóbrega-Pereira S, Gelman D, Bartolini G, Pla R, Pierani A, Marín O. Origin and molecular specification of globus pallidus neurons. J Neurosci. 2010;30(8):2824–34.

22. Medina L, Abellán A, Vicario A, Desfilis E. Evolutionary and developmental contributions for understanding the organization of the basal ganglia. Brain Behav Evol. 2014;83(2): 112–25.

23. Conlee JW, Shapiro SM. Development of cerebellar hypoplasia in jaundiced Gunn rats: a quantitative light microscopic analysis. Acta Neuropathol. 1997;93(5):450–60.

24. Thomson JA, Itskovitz-Eldor J, Shapiro SS, Wants MA, Swiergiel JJ, Marshall VS, Jones JM. Embryonic stem cell lines derived from human blastocysts. Science. 1998;282(5391): 1145–47.

25. Galvin-Burgess KE, Trvis ED, Pierson KE, Vivian JL. TGF-b-superfamily signaling regulates embryonic stem cell heterogeneity: self-renewal as a dynamic and regulated equilibrium. Stem Cells. 2013;31(1):48–58.

26. Kim TG, Yao R, Monnell T, Cho JH, Vasudevan A, Koh A, Kumar PT, Moon M, Datta D, Bolshakov VY, Kim KS, et al. Efficient specification of interneurons from human pluripotent stem cells by dorsoventral and postcaudal modulation. Stem Cells. 2014;32(7):1789–808.

27. Sherwood NM, Timiras PS. A stereotaxic atlas of the developing rat brain. Berkeley (CA): C.W.C. Education Information Center, University of California Press; 1970.

28. Anderson SA, Baraban SC. Cell therapy using GABAergic neural progenitors. In: Noebels JL, Avoli M, Rogawski MA, Olsen RW, Delgado-Escueta AV, editors. Jasper's basic mechanisms of the epilepsies. 4th ed. Bethesda (MD): National Center for Biotechnology Information; 2012:1122–28.

29. Garcia AD, Doan NB, Imura T, Bush TG, Sofroniew MV. GFAP-expressing progenitors are the principal source of constitutive neurogenesis in adult mouse forebrain. Nat Neurosci. 2004;7(11):1233–41.

30. Imura T, Nakano I, Kornblum HI, Sofroniew MV. Phenotypic and functional heterogeneity of GFAP-expressing cells in vitro: differential expression of LeX/CD15 by GFAP-expressing multipotent neural stem cells and non-neurogenic astrocytes. Glia. 2006;53(3):277–93.

31. Liu Y, Namba T, Liu J, Suzuki R, Shioda S, Seki T. Glial fibrillary acidic protein- expressing neural progenitors give rise to immature neurons via early intermediate progenitors expressing both glial fibrillary acidic protein and neuronal markers in the adult hippocampus. Neuroscience. 2010;166(1):241–51.

32. Sedlak TW, Saleh M, Higginson DS, Paul BD, Juluri KR, Snyder SH. Bilirubin and glutathione have complementary antioxidant and cytoprotective roles. Proc Natl Acad Sci. 2009;106(13):5171–76.

33. Liu Y, Li P, Lu J, Xiong W, Oger J, Tetzlaff W, Cynader M. Bilirubin possesses powerful immunomodulatory activity and suppresses experimental autoimmune encephalomyelitis. J Immunol. 2008;181(3):1887–97.

34. Larsson LC, Czech KA, Brundin P, Widner H. Intrastriatal ventral mesencephalic xenografts of porcine tissue in rats: immune responses and functional effects. Cell Transplant. 2000;9(2):261–72.

35. Barker RA, Widner H. Immune problems in central nervous system cell therapy. Neurorx. 2004;1(4):472–81.

36. Gazzin S, Zelenka J, Zdrahalova L, Konickova R, Zabetta CC, Giraudi PJ, Berengeno AL, Raseni A, Robert MC, Vitek L, Tiribelli C. Bilirubin accumulation and Cyp mRNA expression in selected brain regions of jaundiced Gunn rat pups. Pediatr Res. 2012;71(6):653–60.

37. Guillaume DJ, Johnson MA, Li XJ, Zhang SC. Human embryonic stem cell-derived neural precursors develop into neurons and integrate into the host brain. J Neurosci Res. 2006;84(6):1165–76.

38. Kita H. Parvalbumin-immunopositive neurons in rat globus pallidus: a light and electron microscopic study. Brain Res. 1994;657(1–2):31–41.

39. Mallet N, Micklem BR, Henny P, Brown MT, Williams C, Bolam JP, Nakamura KC, Magill PJ. Dichotomous organization of the external globus pallidus. Neuron. 2012;74(6): 1075–86.

40. Oh YM, Karube F, Takahashi S, Kobayashi K, Takada M, Uchigashima M, Watanabe M, Nishizawa K, Kobayashi K, Fujiyama F. Using a novel PV-Cre rat model to characterize pallidonigral cells and their terminations. Brain Struct Funct. 2017;222(5):2359–78.

41. Saunders A, Huang KW, Sabatini BL. Globus pallidus externus neurons expressing parvalbumin interconnect the subthalamic nucleus and striatal interneurons. PLoS ONE. 2016;11(2):e0149798.

42. Hegeman DJ, Hong ES, Hernández VM, Chan CS. The external globus pallidus: progress and perspectives. Eur J Neurosci. 2016;43(10):1239–65.

43. Ruzicka BB, Akil H. The interleukin-1beta-mediated regulation of proenkephalin and opioid receptor messenger RNA in primary astrocyte-enriched cultures. Neuroscience. 1997;79(2):517–24.

44. Hauser KF, Osborne JG, Stiene-Martin A, Melner MH. Cellular localization of proenkephalin mRNA and encephalin peptide products in cultured astrocytes. Brain Res. 1990;522(2):347–53.

45. Melner MH, Low KG, Allen RG, Nielsen CP, Young SL, Saneto RP. The regulation of proenkephalin expression in a distinct population of glial cells. EMBO J. 1990;9(3):791–96.

46. Yang FC, Riordan SM, Winter M, Gan L, Smith PG, Vivian JL, Shapiro SM, Stanford JA. Fate of neural progenitor cells transplanted into jaundiced and nonjaundiced rat brains. Cell Transplant. 2017;26(4):605–11.

47. Casalia ML, Li T, Ramsay H, Ross PJ, Paredes MF, Baraban SC. Interneuron origins in the embryonic porcine medial ganglionic eminence. J Neurosci. 2021;41:3105–19.

48. Romariz SA, Paiva DS, Galindo LT, Barnabé GF, Guedes VA, Borlongan CV, Longo BM. Medial ganglionic eminence cells freshly obtained or expanded as neurospheres show distinct cellular and molecular properties in reducing epileptic seizures. CNS Neurosci Ther. 2017;23(2):127–34.

49. Daadi MM, Lee SH, Arac A, Grueter BA, Bhatnagar R, Maag AL, Schaar B, Malenka RC, Palmer TD, Steinberg GK. Functional engraftment of the medial ganglionic eminence cells in experimental stroke model. Cell Transplant. 2009;18(7):815–26.

50. Martínez-Serrano A, Pereira MP, Avaliani N, Nelke A, Kokaia M, Ramos-Moreno T. Short-term grafting of human neural stem cells: electrophysiological properties and motor behavioral amelioration in experimental Parkinson's disease. Cell Transplant. 2016;25(12):2083–97.

51. Parmar M, Björklund A. Generation of transplantable striatal projection neurons from human ESCs. Cell Stem Cell. 2012;10(4):349–50.

52. Gordeeva OF. Pluripotent cells in embryogenesis and in teratoma formation. J Stem Cells. 2011;6(1):51–63.

53. Brederlau A, Correia AS, Anisimov SV, Elmi M, Paul G, Roybon L, Morizane A, Bergquist F, Riebe I, Nannmark U, Carta M, et al. Transplantation of human embryonic stem cell-derived cells to a rat model of Parkinson's disease: effect of in vitro differentiation on graft survival and teratoma formation. Stem Cells. 2006;24(6):1433–40.